GEOPHYSICAL RESEARCH LETTERS, VOL. 34, L03501, doi:10.1029/2006GL028697, 2007

Evolution of melt pond volume on the surface of the Greenland Ice Sheet

W. A. Sneed[1] and G. S. Hamilton[1]

Received 6 November 2006; revised 29 December 2006; accepted 11 January 2007; published 14 February 2007.

[1] The presence of surface meltwater on ice caps and ice sheets is an important glaciological and climatological characteristic. We describe an algorithm for estimating the depth and hence volume of surface melt ponds using multispectral ASTER satellite imagery. The method relies on reasonable assumptions about the albedo of the bottom surface of the ponds and the optical attenuation characteristics of the ponded meltwater. We apply the technique to sequences of satellite imagery acquired over the western margin of the Greenland Ice Sheet to derive changes in melt pond extent and volume during the period 2001–2004. Results show large intra- and interannual changes in ponded water volumes, and large volumes of liquid water stored in extensive slush zones. **Citation:** Sneed, W. A., and G. S. Hamilton (2007), Evolution of melt pond volume on the surface of the Greenland Ice Sheet, *Geophys. Res. Lett.*, *34*, L03501, doi:10.1029/2006GL028697.

1. Introduction

[2] Ponded surface meltwater (Figure 1) is a well-known phenomenon near the margin of the Greenland Ice Sheet [*Echelmeyer et al.*, 1991; *Jezek et al.*, 1993; *Bryzgis and Box*, 2005] and other Arctic ice caps [*Liestøl et al.*, 1980]. Topographic depressions in the ice surface exert a first-order control on lake location, with ponds and lakes tending to form in the same depressions in successive summers [*Echelmeyer et al.*, 1991]. After formation, lake evolution is governed by a positive albedo-feedback mechanism, in which the lower albedo of surface waters enhances radiative-driven melting [*Lüthje*, 2005]. Variations in the distribution and number of ponds with time represent changes in the surface climate conditions which control melting. The fluctuating availability of large volumes of ponded surface water raises the possibility of sudden drainage to the bed, a change in basal lubrication, and a rapid increase in ice velocity [*Zwally et al.*, 2002; *Parizek and Alley*, 2003; *Boon and Sharp*, 2003]. Recent studies have also linked the rapid collapse of small ice shelves fringing the Antarctic Peninsula to the progressive development of surface melt ponds [*Scambos et al.*, 2000].

[3] While the problem of calculating the areal extent of meltwater ponds using satellite imagery is fairly straightforward [*Lüthje*, 2005], determining the depth and thus their volume is not. Here, we develop a technique for estimating melt pond depth using multispectral satellite imagery acquired by the Advanced Spaceborne Thermal Emission and Reflection Radiometer (ASTER). The technique is applied to images collected over Kong Oscar Gletscher, an ice sheet outlet glacier in NW Greenland that flows into Melville Bay at 75°59′N and 50°48′W, to calculate the volumes of water stored in ponds, lakes, and the saturated snow of the glacier surface. Our results reveal large quantities of ponded water and rapid changes in pond volume at monthly and interannual time scales.

2. Method Development

2.1. Theoretical Basis

[4] Determining water depth, bottom or substrate albedo, and the optical properties of the water column using remotely-sensed visible wavelength imagery has long been a goal of oceanographers and limnologists. Many of the methods proposed for determining depth and albedo are based on some form of the Bouguer-Lambert-Beer law

$$L(z, \lambda) = L(0, \lambda)e^{-(K_\lambda)(z)} \quad (1)$$

where $L(z, \lambda)$ is the water-leaving spectral radiance at some depth, $L(0, \lambda)$ is the spectral radiance at zero depth, K_λ is the spectral attenuation, and z is depth. For the remainder of this note we will forego the use of the adjective, spectral, and the argument, λ, for brevity's sake. All variables with the exception of depth are wavelength-dependent.

[5] Written in terms of reflectance, inverted to logarithmic form, and solved for z [*Philpot*, 1989]

$$z = (\ln(A_d - R_\infty) - \ln(R_w - R_\infty))/(-g) \quad (2)$$

where A_d is the bottom or substrate albedo (reflectance), R_∞ is the reflectance for optically deep water, and R_w is the reflectance at some depth. The quantity g is

$$g \approx K_d + aD_u \quad (3)$$

where K_d is the diffuse attenuation coefficient for downwelling light, a is the beam absorption coefficient, and D_u an upwelling light distribution function or the reciprocal of the upwelling average cosine [*Mobley*, 2004]. When scattering within the water column is low, *Philpot* [1989] suggests $1.5\ K_d < g < 3\ K_d$, with larger values being used as scattering increases. *Maritorena et al.* [1994] use a value for g of $2\ K_d$ but warn that it underestimates actual attenuation. Such an underestimation will lead to an overestimation of depth, z, in equation (2) [*Philpot*, 1989].

2.2. Assumptions

[6] The only data we have available for analysis is the signal leaving the water's surface, transiting the atmosphere, and arriving at the satellite sensor. This complex signal

[1]Climate Change Institute, University of Maine, Orono, Maine, USA.

0094-8276/07/2006GL028697$05.00

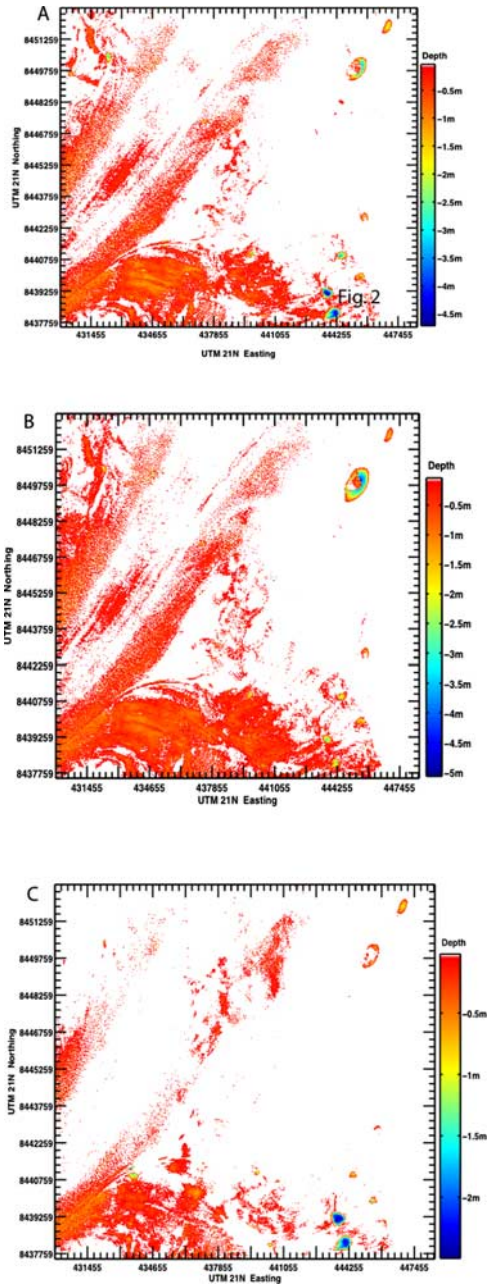

Figure 1. Meltwater depths derived using equation (2) overlaid on ASTER images acquired on (a) 29 June 2003 (b) 06 July 2003, and (c) 08 July 2004.

contains within it information about substrate reflectance, water depth, and any dissolved or suspended materials within the water column [*Bierwirth et al.*, 1993]. In our analysis we make the following assumptions:

[7] 1. The substrate of a melt pond is homogeneous.

[8] 2. Suspended or dissolved organic or inorganic particulate matter is minimal.

[9] 3. There is no inelastic scattering, e.g., Raman scattering or fluorescence.

[10] 4. There is no wind and, thus, no waves on a pond's surface.

[11] *Hedley and Mumby* [2003] point out that if a depth estimation is sought a valid assumption must be made about either the bottom albedo or the uniformity and homogeneity of the substrate material. Therefore, whether for a small melt pond in a crevasse field near a glacier's terminus or a large melt lake formed in a topographic depression farther upglacier, we assume that the substrate is everywhere ice and the albedo the same throughout. For a first approximation of depth calculated by the proposed method we further assume that the bottom for any given pixel is parallel to the water surface. Small melt ponds in steep-sided crevasses most likely do not have surface-parallel bottoms, so our method will need modification before use in these situations.

[12] We will assume that the melt water is pure natural fresh water with the absorption and scattering coefficients, a_w and b_m respectively, reported by *Smith and Baker* [1981].

[13] Small melt ponds found in the heavily crevassed regions of a glacier are likely to be well-sheltered from the effects of wind by the crevasse walls. Larger bodies of melt water found farther inland on an ice sheet are undoubtedly affected by katabatic winds. The remotely-sensed reflectance depends, in part, on the wavelength and amplitude of surface waves [*Zaneveld et al.*, 2001] but lacking wind speed and wave amplitude and period data we assume water surfaces to be flat.

2.3. Method

[14] The ASTER images used in this study are atmospherically corrected, surface reflectance scenes either created in-house from Level L1A scenes or available as ASTER On-Demand L2 Surface Reflectance products from the Land Processes Distributed Active Archive (LPDAAC) at http://edcimswww.cr.usgs.gov/pub/imswelcome. In either case we use only ASTER bands VNIR1 (520–600 nm) and VNIR3N (780–860 nm) which have a 15 m pixel resolution. VNIR1 is used to solve equation (2) for water depth, z, on a pixel-by-pixel basis and VNIR3N is used to determine the bottom albedo, A_d.

[15] As a practical matter, R_∞, reflectance over optically deep water where the influence of bottom reflectance is nil, can be derived from water that is deeper than ~40 m. We are thus restricted to images that contain some open ocean water that is clear of sea ice, meltwater plumes, and sun glint. Ideally, we seek images with deep water far from shore because the absorption and scattering effects of suspended particulates are minimized.

[16] Several researchers [*Leathers and McCormick*, 1999; *Chang et al.*, 2003] note the difficulties involved in obtaining in situ bottom reflectance values. A common solution [*Maritorena et al.*, 1994; *Legleiter et al.*, 2004] is to bring a sample of bottom material to the surface, wet it, and measure the reflectance. In a process somewhat analogous to this, we use the near-infrared band, VNIR3N, to find the pixels at a pond's edge that are just barely covered with water. By equation (1) it can be shown that at 780 nm with 10 cm of water covering ice, the above-water measured reflectance will be about 40% less than the reflectance of ice with no water cover. Thus by searching for adjacent pixels that show a rapid decrease in the reflectance as measured at the satellite sensor in band VNIR3N and then finding the same pixels in the VNIR1 image we can arrive at a value for the bottom albedo, A_d, needed in equation (2).

[17] To determine a value for g in equation (2), we average the a_w and b_m values [*Smith and Baker*, 1981] for

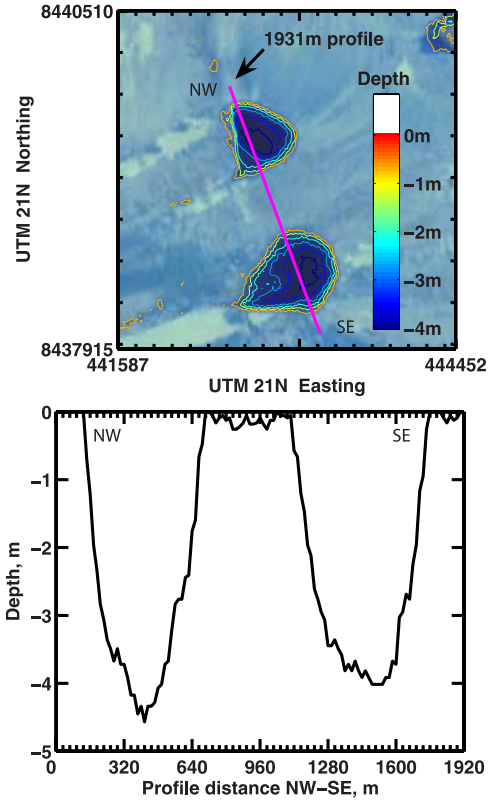

Figure 2. Depth contours and pond profiles, Kong Oscar Gletscher, 29 June 2003 for the ponds in the lower right of Figure 1a.

the VNIR1 band, solve their equality, $K \geq a_w + 1/2\ b_m$, for K and set $g = 2\ K$ [*Maritorena et al.*, 1994].

3. Results and Discussion

[18] We apply the model to sequences of ASTER satellite imagery (Figure 1) acquired over the western margin of the Greenland Ice Sheet with encouraging results. Estimates of water depth derived from equation (2) for two melt ponds (lower right corner of Figure 1a) are shown in Figure 2. The contoured depths of the ponds (Figure 2, top) are consistent with water-filled surface depressions comprised of an annulus of shallow water and rapidly deepening water towards the center. The profile in Figure 2 (bottom) shows the maximum water depths along the profile line but not necessarily the maximum depth of the ponds. Results indicate that surface ponds can reach depths of several meters. We have yet to conduct direct validation of our derived pond depths with field measurements. However, the range of obtained depths is consistent with published reports of measured pond depths. *Liestøl et al.* [1980] describe an emptied surface lake on Brøggerbreen, Svalbard, with a length of ~200 m and a maximum depth of ~10 m. *Echelmeyer et al.* [1991] report on a number of surface lakes in the upper portion of Jakobshavns Isbræ drainage basin with surface areas from a few tens of square meters up to 10 km^2 and depths ranging from <1 m to 20 m in crevasses.

[19] Melt ponds on the surface of Kong Oscar Gletscher undergo a rapid seasonal evolution according to our analysis of two ASTER images collected eight days apart in June and July of 2003 (Figures 1a and 1b and Table 1). During this period, wetted surface area and water volume increase by ~20%. The two ponds in the lower right corner of Figures 1a and 1b (elevation ~650 m) decrease in depth and extent, while the large pond in the upper right corner (elevation ~820 m) increases in both depth and extent. We interpret this change in pond volumes as being due to the progression of summer warming to higher elevations where snow melts rapidly to supply growing ponds. At lower elevations, existing ponds do not grow as rapidly, or they drain through surface outlet streams or cracks in the ice (the low elevation ponds in Figure 2 are close to crevasses).

[20] The inter-annual changes are even greater, with a five-fold decrease in wetted surface area and water volume between July 2003 and July 2004 (Figures 1a and 1c and Table 1). Many of the ponds remained fixed in space indicating that their position is controlled by surface topography. The smaller pond volumes in July 2004 are consistent with the delayed onset of melting in summer 2004, inferred from cooler temperatures recorded at nearby coastal weather stations in May/June/July 2004 relative to the same months a year earlier. (Data for Upernavik and Qaanaaq available from Danmarks Meteorologiske Institut, http://www.dmi.dk/dmi/index/gronland/vejrarkiv-gl.htm.)

[21] Much of the intra- and inter-annual change in water extent and volume is due to changes in shallow ($z \leq 1.5$ m) liquid water on the glacier surface. In the 29 June 2003 image (Figure 1a), approximately 88% of the total volume of meltwater is between 20 cm and 1.5 m deep, in the 06 July 2003 image (Figure 1b) the percentage is ~91%, and in the 08 July 2004 image (Figure 1c) the percentage is ~83%.

[22] This pattern indicates that surface meltwater storage is not limited to the development of large ponds, although it is likely that some of the non-ponded water drains into ponds. These results point to the value of our technique for detecting and quantifying liquid water of varying depth on snow and ice surfaces.

[23] Prominent in Figures 1a–1c are the liquid water-free areas (the right hand edge) and the fairly abrupt transition to areas with shallow liquid water. This transition may mark a line that has been variously called the run-off limit [*Braithwaite et al.*, 1994] or the maximum slush line [*Greuell and Knap*, 2000]. Above this line the snow is deep enough so that any meltwater penetrates deeply into the snow creating wet snow but the snowpack does not become saturated forming slush [*Greuell and Knap*, 2000]. Below the maximum slush line *Braithwaite et al.* [1994] suggest that the firn can be no deeper than a few meters for run-off of meltwater to occur and it is probably underlain by an near-surface ice layer [*Greuell and Knap*, 2000].

[24] The results shown Table 1 are most sensitive to the value chosen for A_d (equation (2)) in which a ~1% decrease

Table 1. Meltwater Area and Volume for the Images Shown in Figure 1

Date	Total Area, km^2	Area Meltwater, km^2	Volume Meltwater, m^3	Figure
29 June 2003	265	40.7	2.2×10^7	1a
06 July 2003	265	48.7	2.66×10^7	1b
08 July 2004	265	10.1	4.35×10^6	1c

in the bottom albedo results in a ~16% decrease in calculated meltwater volume. Accumulation of organic or inorganic matter at the bottom of a melt pond would decrease the bottom albedo while sun glint caused by surface waves would have the effect of increasing the observed bottom albedo. The volume calculations are less sensitive to changes in the values of g and R_∞; a ~10% decrease in g produces a ~10% calculated volume increase while a ~2% increase in R_∞ results in a ~0.5% increase in calculated volume. It is difficult to improve R_∞ other than to exercise care when choosing the "blackest" deep water pixels.

[25] Preliminary laboratory analysis of melt pond water samples taken from Helheim Glacier, East Greenland in July and August 2006 justifies our assumption of little organic or inorganic particulates. Total suspended solids were 0.74 mgL^{-1} and 0.20 mgL^{-1} for the July and August samples, respectively. Chlorophyll-*a* was measured for only the July meltwater sample and was found to be just above the instrumental detection limit but was based on a relatively small sample volume (~1 L). A more detailed laboratory analysis of the absorption and scattering properties of meltwater samples will further constrain g. Additional refinement of g may be possible using HYDROLIGHT® (Sequoia Scientific, Inc., Bellevue, WA, USA), a radiative transfer numerical modeling software package. Reducing the uncertainties of A_d is much more problematic without some in situ instrumental measurements although it may be possible to refine A_d using a ratio of VNIR1 (520–600 nm) and VNIR2 (630–690 nm) as suggested by *Lyzenga* [1978].

4. Conclusion

[26] We describe a radiative transfer model for estimating the volume of meltwater stored in ponds on the surface of ice sheets and ice caps. The model is applied to multispectral ASTER satellite imagery of Greenland. Initial results show that, while the method is sensitive to assumptions about bottom albedo and water quality, reasonable values for pond geometry and depth are obtained. We show that the melt pond depths and water volume evolve rapidly during an eight day period. Interannual changes in surface water extent and volume are also noted. We note large areas of non-ponded surface water and their major contribution to the total meltwater volume. Although our derived depths have not yet been validated with direct field measurements, our values are consistent with published reports of pond depths elsewhere in Greenland and in Svalbard.

[27] The generation and ponding of meltwater on ice sheet surfaces raises the possibility of its sudden drainage to the bed and a rapid change in basal lubrication [*Zwally et al.*, 2002; *Parizek and Alley*, 2003; *Boon and Sharp*, 2003]. Our algorithm is a potentially useful tool for monitoring the evolution of surface meltwater on ice sheets and ice caps, with a view to understanding the role of surface water in ice flow dynamics.

[28] **Acknowledgments.** This work was supported by awards from NASA (Cryospheric Sciences Program) and NSF (Arctic Natural Sciences) to GSH, and a Maine Space Grant Consortium award to WAS. We appreciate the constructive comments from two anonymous reviewers.

References

Bierwirth, P. N., T. J. Lee, and R. V. Burne (1993), Shallow sea-floor reflectance and water depth derived by unmixing multispectral imagery, *Photogramm. Eng. Remote Sens.*, *59*(3), 331–338.

Boon, S., and M. Sharp (2003), The role of hydrologically-driven ice fracture in drainage system evolution on an Arctic glacier, *Geophys. Res. Lett.*, *30*(18), 1916, doi:10.1029/2003GL018034.

Braithwaite, R. J., M. Laternser, and W. T. Pfeffer (1994), Variations of near-surface firn density in the low accumulation area of the Greenland ice sheet, Påkitsoq, West Greenland, *J. Glaciol.*, *40*(136), 477–485.

Bryzgis, G., and J. E. Box (2005), West Greenland ice sheet melt lake observations and modeling, *Eos Trans. AGU*, *86*(52), Fall Meet. Suppl., Abstract C41A-07.

Chang, G. C., T. D. Dickey, C. D. Mobley, E. Boss, and W. S. Pegau (2003), Toward closure of upwelling radiance in coastal waters, *Appl. Opt.*, *42*(9), 1574–1582.

Echelmeyer, K., T. Clarke, and W. Harrison (1991), Surficial glaciology of Jakobshavns Isbræ, West Greenland: Part I. Surface morphology, *J. Glaciol.*, *37*(127), 368–382.

Greuell, W., and W. H. Knap (2000), Remote sensing of the albedo and detection of the slush line on the Greenland ice sheet, *J. Geophys. Res.*, *105*(D12), 15,567–15,576.

Hedley, J. D., and P. J. Mumby (2003), A remote sensing method for resolving depth and subpixel composition of aquatic benthos, *Limnol. Oceanogr.*, *48*(1), 480–488.

Jezek, K., M. Drinkwater, J. Crawford, R. Bindschadler, and R. Kwok (1993), Analysis of synthetic aperture radar data collected over the southwestern Greenland ice sheet, *J. Glaciol.*, *39*(131), 119–132.

Leathers, R. A., and N. J. McCormick (1999), Algorithms for ocean-bottom albedo determination from in-water natural-light measurements, *Appl. Opt.*, *38*(15), 3199–3205.

Legleiter, C. J., D. A. Roberts, W. A. Marcus, and M. A. Fonstad (2004), Passive optical remote sensing of river channel morphology and in-stream habitat: Physical basis and feasibility, *Remote Sens. Environ.*, *93*, 493–510.

Liestøl, O., K. Repp, and B. Wold (1980), Supra-glacial lakes in Spitsbergen, *Nor. Geogr. Tidsskr.*, *34*, 89–92.

Lüthje, M. (2005), Modelling drainage processes, a numerical and remote sensing investigation of pond formation on ice surfaces, Ph.D. thesis, Tech. Univ. of Den., Lyngby, Denmark.

Lyzenga, D. R. (1978), Passive remote sensing techniques for mapping water depth and bottom features, *Appl. Opt.*, *17*(3), 379–383.

Maritorena, S., A. Morel, and B. Gentili (1994), Diffuse reflectance of oceanic shallow waters: Influence of water depth and bottom albedo, *Limnol. Oceanogr.*, *39*(7), 1689–1703.

Mobley, C. D. (2004), *Light and Water: Radiative Transfer in Natural Waters* [CD-ROM], edited by C. D. Mobley, Elsevier, New York.

Parizek, B., and R. Alley (2003), Implications of increased Greenland surface melt under global-warming scenarios: Ice-sheet simulations, *Quat. Sci. Rev.*, *23*, 1013–1027.

Philpot, W. D. (1989), Bathymetric mapping with passive multispectral imagery, *Appl. Opt.*, *28*(8), 1569–1578.

Scambos, T., C. Hulbe, and M. Fahnestock (2000), The link between climate warming and break-up of ice shelves in the Antarctic Peninsula, *J. Glaciol.*, *46*(154), 516–530.

Smith, R. C., and K. S. Baker (1981), Optical properties of the clearest natural waters (200–800 nm), *Appl. Opt.*, *20*(2), 177–184.

Zaneveld, J. R. V., E. Boss, and P. A. Hwang (2001), The influence of coherent waves on the remotely sensed reflectance, *Opt. Express*, *9*(6), 260–266.

Zwally, H., W. Abdalati, T. Herring, K. Larson, J. Saba, and K. Steffen (2002), Surface melt induced acceleration of Greenland Ice Sheet flow, *Science*, *297*, 218–222.

G. S. Hamilton and W. A. Sneed, Climate Change Institute, University of Maine, Sawyer Environmental Research Building, Orono, ME 04469, USA. (william.sneedjr@maine.edu)